photonics

MDPI

Supplementary Material of Improved Classification of Blurred Images with Deep Learning Networks Using Lucy-Richardson-Rosen Algorithm

Amudhavel Jayavel [1,†], Shivasubramanian Gopinath [1,†], Praveen Periyasamy Angamuthu [1,†], Francis Gracy Arockiaraj [1], Andrei Bleahu [1], Agnes Pristy Ignatius Xavier [1], Daniel Smith [2], Molong Han [2], Ivan Slobozhan [3], Soon Hock Ng [2], Tomas Katkus [2], Aravind Simon John Francis Rajeswary [1], Rajesh Sharma [3], Saulius Juodkazis [2,4] and Vijayakumar Anand [1,2,*]

[1] Institute of Physics, University of Tartu, W. Ostwaldi 1, 50411 Tartu, Estonia; amudhavel.jayavel@ut.ee (A.J.); shivasubramanian.gopinath@ut.ee (S.G.); praveen@ut.ee (P.P.A.); francis.gracy.arockiaraj@ut.ee (F.G.A.); andrei-ioan.bleahu@ut.ee (A.B.); agnes.pristy.ignatius.xavier@ut.ee (A.P.I.X.); aravind@ut.ee (A.S.J.F.R.)

[2] Optical Sciences Center, Swinburne University of Technology, Melbourne 3122, Australia; danielsmith@swin.edu.au (D.S.); molonghan@swin.edu.au (M.H.); soonhockng@swin.edu.au (S.H.N.); tkatkus@swin.edu.au (T.K.); sjuodkazis@swin.edu.au (S.J.)

[3] Institute of Computer Science, University of Tartu, 51009 Tartu, Estonia; ivan.slobozhan@ut.ee (I.S.); rajesh.sharma@ut.ee (R.S.)

[4] Tokyo Tech World Research Hub Initiative (WRHI), School of Materials and Chemical Technology, Tokyo Institute of Technology, 2-12-1, Ookayama, Meguro-ku, Tokyo 152-8550, Japan

* Correspondence: vijayakumar.anand@ut.ee (V.A.)

† These authors contributed equally to this work.

Deep Learning Pre-Trained Networks (DLPTN) used in this study

S. No	Pre-Trained Model	Acronym
1	DARKNET53	DN53
2	EFFICIENTNETB0	EFNETB0
3	INCEPTIONRESNETV2	IRV2
4	NASNETLARGE	NNL
5	NASNETMOBILE	NNMB
6	RESNET101	RS101
7	RESNET50	RN50
8	DARKNET53	DN53
9	EFFICIENTNETB0	EFNETB0
10	INCEPTIONRESNETV2	IRV2
11	NASNETMOBILE	NNMB
12	RESNET101	RS101
13	RESNET50	RN50
14	EFFICIENTNETB0	EFNETB0
15	INCEPTIONRESNETV2	IRV2
16	NASNETLARGE	NNL
17	RESNET101	RS101
18	RESNET50	RN50

In the supplementary section, a different approach was used to evaluate the performance of LR^{2}A with respect to LRA and NLR. In the main document, the classification probability was obtained for different cases and compared. In the supplementary section, all the above 18 DLPTNs were used for different cases of aberrations and the total number of

Citation: To be added by editorial staff during production.

Received: date
Revised: date
Accepted: date
Published: date

successful classification of "Bell pepper" by the pre-trained deep-learning networks were calculated. This number of successful classification is called hits.

Deep Learning Experiments

The supplementary section encapsulates the outcomes of an investigative trial wherein the imaging condition was perturbed by shifting the object distance (Delta) in millimeters, and the hit count was documented. For every Delta value, the mean, standard deviation (STD), minimum (Min), lower quartile (LQ), middle quartile (MQ) or median, upper quartile (UQ), and maximum (Max) hit count was counted. The values were calculated by the conventional descriptive statistical analysis method.

Here, D-25, D-50, D-75, D-100 represent the different axial aberration values (Δz) ranging from 25 mm to 100 mm with an increment of 25 mm. The values corresponding to the different radii of the aperture ranges from 50 pixels to 300 pixels with the increment of 25 pixels. The design wavelengths associated with the axial aberration ranges from 400 nm to 700 nm with the increment of 50 nm.

Table S1: Statistical Analysis of Delta Values with respect to NLR

Δz	Hits	Mean	STD	Min	LQ	MQ	UQ	Max
D-25	64	21.2	11.2	5.6	12	19.5	31	37.8
D-50	96	18.3	7.3	8.6	10.9	17.2	24.8	29
D-75	152	20.2	16.5	7.1	8.2	12.3	26.6	59
D-100	248	25.1	23.8	6.8	9.4	10.1	55.4	73

These statistical findings in Figs. S1-S4 reveal a collection of the hit values for each deblurring methodologies. The statistical analysis from Table S1, 2, and 3 shows that the NLR method gained the most meager mean hit value of 140, sporting a broad standard deviation of 72.53. The hit values ranged from 64 to 248, with the first quartile (Q1) at 80, the median at 124, and the third quartile (Q3) at 184. The LRA method had a more noteworthy mean hit value of 228, along with a reduced standard deviation of 35.47. The hit values ranged from 176 to 272, with Q1 at 192, median at 232, and Q3 at 256. The LR²A method had the most impressive mean hit value of 250. The hit values ranged from 240 to 256, with Q1 at 248, median at 248, and Q3 at 256.

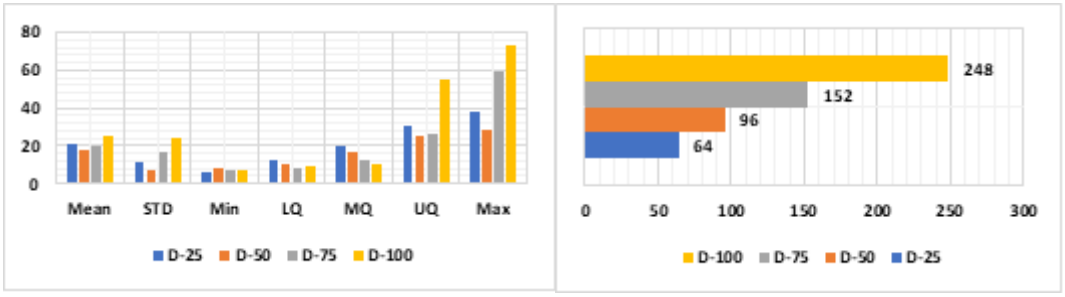

Figure S1: Performance Comparison of Delta/No. of Hits.r.t NLR

Table S2: Statistical Analysis of Delta Values with respect to LRA

Δz	Hits	Mean	STD	Min	LQ	MQ	UQ	Max
D-25	176	37.1	24.9	11.2	17.4	22.7	60.6	80.3
D-50	208	39.7	26.6	7.4	14.4	32.2	75.3	83

D-75	256	43.6	26.5	12.8	16.7	38.9	78.8	82.9
D-100	272	41.3	26.7	13.3	15.2	37.2	78.6	81.8

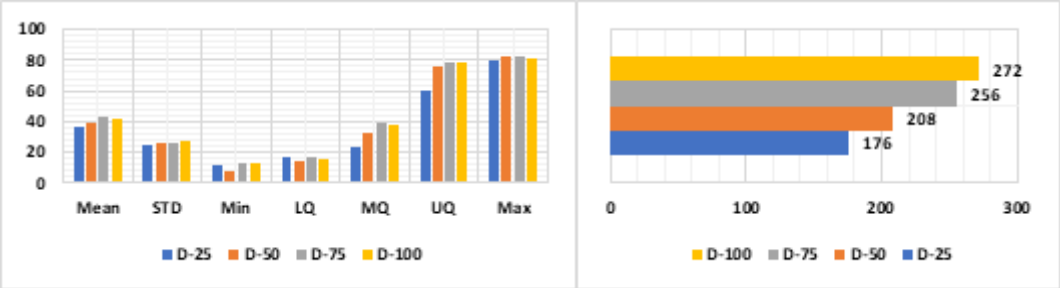

Figure S2: Performance Comparison of Delta/No. of Hits.r.t LRA

Table S3: Statistical Analysis of Delta Values with respect to LR²A

Δz	Hits	Mean	STD	Min	LQ	MQ	UQ	Max
D-25	240	38	24.6	7.9	17	31.7	56.9	84.7
D-50	256	41.9	27.4	8.4	15.4	35.2	75.5	86.7
D-75	256	37.1	26.5	9.3	13.1	31.2	66.9	82.1
D-100	248	37.4	26.1	10.6	12.8	32.4	74.6	81.1

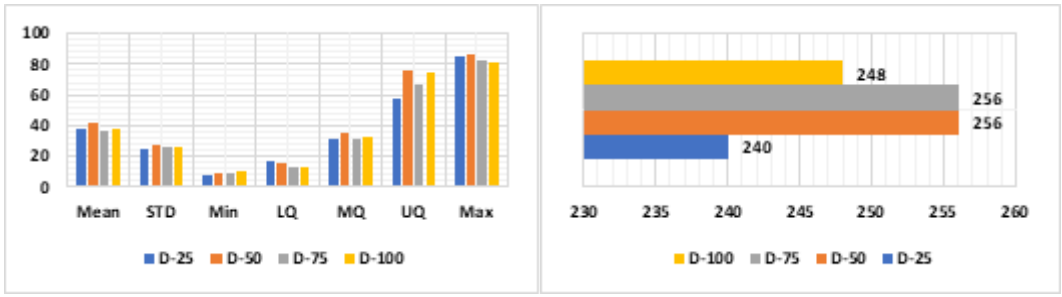

Figure S3: Performance Comparison of Delta/No. of Hits.r.t LR²A

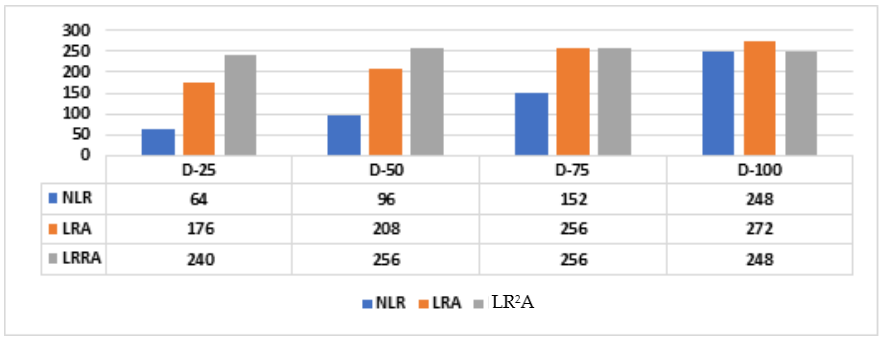

Figure S4: Performance comparison of NLR, LRA, LR²A with respect to Delta

The performance when the different radii of the aperture ranged from 50 pixels to 300 is presented next. The axial aberration associated with the aperture radii ranges from 25 mm to 100 mm with an increment of 25 mm. The design wavelengths associated with the axial aberration ranges from 400 nm to 700 nm with the increment of 50 nm. P50 corresponds to a radii of 50 pixels.

Table S4: Statistical Analysis of PSF Values with respect to NLR

Radii	Hits	Mean	STD	Min	LQ	MQ	UQ	Max
P50	40	29.8	5.2	24.9	25.7	26.6	33.9	37.8
P75	40	22.2	2.1	19.2	20.7	22.2	24.3	24.8
P100	80	11.8	4.5	4.8	9.4	11.3	12.5	21.6
P125	88	21.9	18.9	5.6	7.4	9.2	47.8	55.4
P150	88	22.4	21.9	7.3	8.6	9.6	30.2	73
P175	64	25.6	21.7	8.1	8.3	13.8	37.9	67.4
P200	48	27.2	21.8	7.8	9.9	19	39.4	68.2
P225	56	21.3	20.8	7.1	9	13.5	24.8	70
P250	40	23.7	21.9	9.4	10	15.5	17	66.6
P275	32	24.1	20.8	10	11.7	13.4	25.7	59.5
P300	32	25.1	18.6	8.8	12.7	18	30.5	55.7

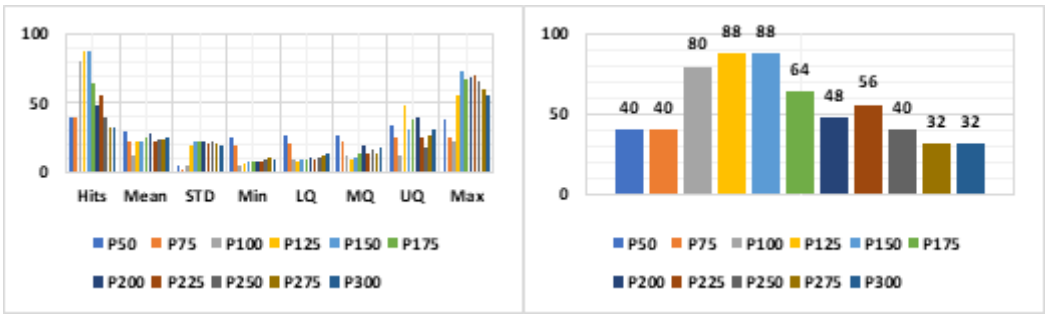

Figure S5: Performance Comparison of Hits with respect to NLR

Table S5: Statistical Analysis of PSF Values with respect to LRA

PSF	Hits	Mean	STD	Min	LQ	MQ	UQ	Max
P50	80	11.8	4.5	4.8	9.4	11.3	12.5	21.6
P75	88	21.9	18.9	5.6	7.4	9.2	47.8	55.4
P100	88	22.4	21.9	7.3	8.6	9.6	30.2	73
P125	64	25.6	21.7	8.1	8.3	13.8	37.9	67.4
P150	48	27.2	21.8	7.8	9.9	19	39.4	68.2
P175	56	21.3	20.8	7.1	9	13.5	24.8	70
P200	40	23.7	21.9	9.4	10	15.5	17	66.6
P225	32	24.1	20.8	10	11.7	13.4	25.7	59.5
P250	32	25.1	18.6	8.8	12.7	18	30.5	55.7
P275	40	29.8	5.2	24.9	25.7	26.6	33.9	37.8
P300	40	22.2	2.1	19.2	20.7	22.2	24.3	24.8

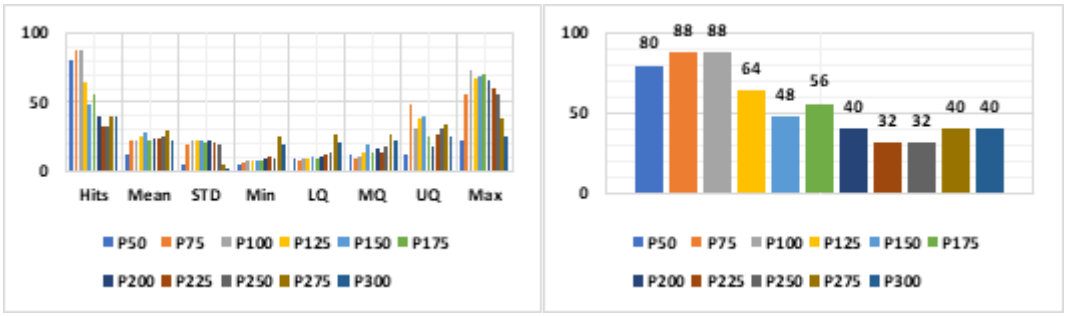

Figure S6: Performance Comparison of Hits with respect to LRA

Table S6: Statistical Analysis of PSF Values with respect to LR²A

PSF	Hits	Mean	STD	Min	LQ	MQ	UQ	Max
P50	8	15.8	15.8	15.8	15.8	15.8	15.8	15.8
P75	72	18.8	12.2	7.9	9.4	12.7	28	39.7
P100	136	36.2	23	13.2	17	26.7	51.1	77.2
P125	136	38.5	26.2	11.8	15.1	31.5	74.3	81.6
P150	128	42.3	26.8	12.6	15.6	38.4	76.5	81.7
P175	120	45.1	28.2	11.2	12.9	37.2	77.6	82.9
P200	144	35.7	23.6	11.6	15.5	32.5	56.9	79.6
P225	128	46	26.6	9.9	21.3	46.6	71.2	84.7
P250	120	42	28	10.7	14	34.1	78.1	86.7
P275	120	43.7	27.2	8.3	23	35.1	78.4	82.1
P300	112	36.5	25.4	8.4	15.5	23.7	66.2	77.8

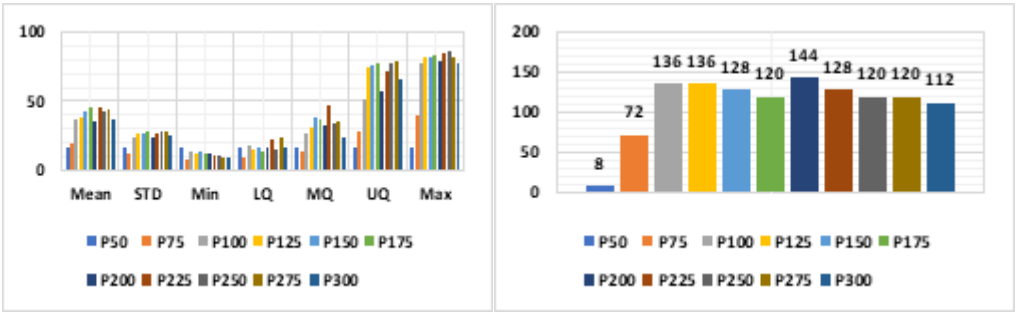

Figure S7: Performance Comparison of Hits with respect to LR²A

Taken together, these performance analysis figures S5, S6, and S7 suggest that the LR²A method evinced the most optimal performance in terms of hit values. The LR²A method likewise shone brightly, boasting a higher mean than NLR and a smaller standard deviation than both NLR and LRA. The NLR method, conversely, suffered the lowest mean and the widest standard deviation, indicating a lesser degree of consistency in performance across the delta values.

The utilization of image quality metrics plays a pivotal role in the evaluation of digital image quality, especially in the field of optics where the accuracy and quality of images are of utmost importance. Numerous metrics are available to quantify the image quality, such as pSNR, SSIM, FSIM, VIF, and RMSE, with each metric offering a distinct perspective on the image quality assessment, enabling us to assess the diverse facets of

image quality. We utilized the power of the above-mentioned metrics to validate the effectiveness of the system.

Table S7: Statistical analysis of peak signal-to-noise ratio (PSNR) with respect to deblurring

PSNR	Range/Values	Mean	STD	Min	LQ	MQ	UQ	Max
LR²A	P100	17.74854	0.091352	17.6269	17.6883	17.739	17.8004	17.8881
	P125	17.76634	0.101549	17.6558	17.6769	17.7278	17.8778	17.8934
	P150	17.70294	0.039991	17.669	17.6799	17.6853	17.7014	17.7791
	P175	17.65704	0.107786	17.4559	17.6727	17.674	17.7144	17.7682
	P200	17.73004	0.071905	17.6064	17.715	17.7295	17.7989	17.8004
	P225	17.69528	0.14212	17.4332	17.6963	17.7141	17.8099	17.8229
	P25	16.05172	0.175861	15.7778	15.9927	16.0378	16.148	16.3023
	P250	17.75808	0.10512	17.6554	17.6708	17.7353	17.7852	17.9437
	P275	17.61372	0.171143	17.3811	17.4425	17.6908	17.7731	17.7811
	P300	17.5467	0.232194	17.1965	17.3684	17.6352	17.7233	17.8101
	P50	17.57936	0.139726	17.4034	17.4446	17.593	17.6984	17.7574
	P75	17.82424	0.312741	17.3983	17.5188	17.9671	18.0533	18.1837
LRA	P100	17.6985	0.087683	17.5828	17.6076	17.7396	17.7663	17.7962
	P125	17.71916	0.039808	17.6421	17.727	17.7337	17.7434	17.7496
	P150	17.69312	0.012488	17.669	17.6946	17.699	17.7007	17.7023
	P175	17.73666	0.186246	17.4916	17.697	17.7048	17.7271	18.0628
	P200	17.71176	0.330071	17.1534	17.7021	17.7035	17.8369	18.1629
	P225	17.68822	0.18987	17.3383	17.7018	17.7085	17.8091	17.8834
	P25	15.74872	0.229865	15.3993	15.5947	15.7824	15.9714	15.9958
	P250	17.75864	0.23908	17.3589	17.7046	17.7506	17.9216	18.0575
	P275	17.33148	0.503872	16.4422	17.1336	17.6214	17.6759	17.7843
	P300	17.38022	0.477727	16.4752	17.4165	17.5268	17.6707	17.8119
	P50	17.34076	0.221501	17.0116	17.2622	17.2938	17.4704	17.6658
	P75	17.7701	0.129552	17.6164	17.6508	17.7934	17.8167	17.9732
NLR	P100	15.94376	0.027169	15.8995	15.9282	15.9539	15.9631	15.9741
	P125	15.86102	0.13376	15.6198	15.8201	15.9316	15.9663	15.9673
	P150	15.72036	0.259741	15.2828	15.5921	15.8145	15.9352	15.9772
	P175	15.54926	0.393462	14.8981	15.3546	15.6504	15.8701	15.9731
	P200	15.33504	0.594791	14.2968	15.1545	15.4789	15.7839	15.9611
	P225	15.12146	0.765164	13.8022	14.8447	15.3336	15.6819	15.9449
	P25	12.92562	0.412457	12.3489	12.6348	12.9288	13.2189	13.4967
	P250	14.8652	0.984277	13.2202	14.3649	15.2423	15.5745	15.9241
	P275	14.71732	1.109914	12.8911	14.0948	15.1682	15.5114	15.9211
	P300	14.66412	1.116753	12.911	13.9053	15.1126	15.4717	15.92
	P50	15.59262	0.090502	15.4588	15.5352	15.5988	15.6572	15.7131
	P75	15.89214	0.053975	15.8192	15.8506	15.8916	15.9332	15.9661

LR²A	D-25	17.54262	0.401266	16.3023	17.55305	17.65045	17.72442	17.9437
	D-50	17.51184	0.460782	16.148	17.39783	17.67385	17.7359	17.9671
	D-75	17.62915	0.509218	15.9927	17.68195	17.7333	17.8212	18.0533
	D-100	17.63333	0.576956	15.7778	17.70758	17.76525	17.8133	18.1837
LRA	D-25	17.50261	0.537048	15.9714	17.32718	17.6599	17.78728	18.0628
	D-50	17.49096	0.56874	15.7824	17.37792	17.73525	17.79733	17.9216
	D-75	17.53038	0.598383	15.5947	17.61175	17.70345	17.74985	17.9732
	D-100	17.50658	0.640409	15.3993	17.66948	17.6994	17.70378	17.8167
NLR	D-25	14.99195	0.871531	13.2189	14.29738	15.25455	15.69793	15.9631
	D-50	15.34378	0.787729	12.9288	15.22378	15.53885	15.83378	15.9741
	D-75	15.48088	0.880195	12.6348	15.52925	15.7329	15.88638	15.9673
	D-100	15.59524	0.993479	12.3489	15.8948	15.92615	15.9624	15.9772

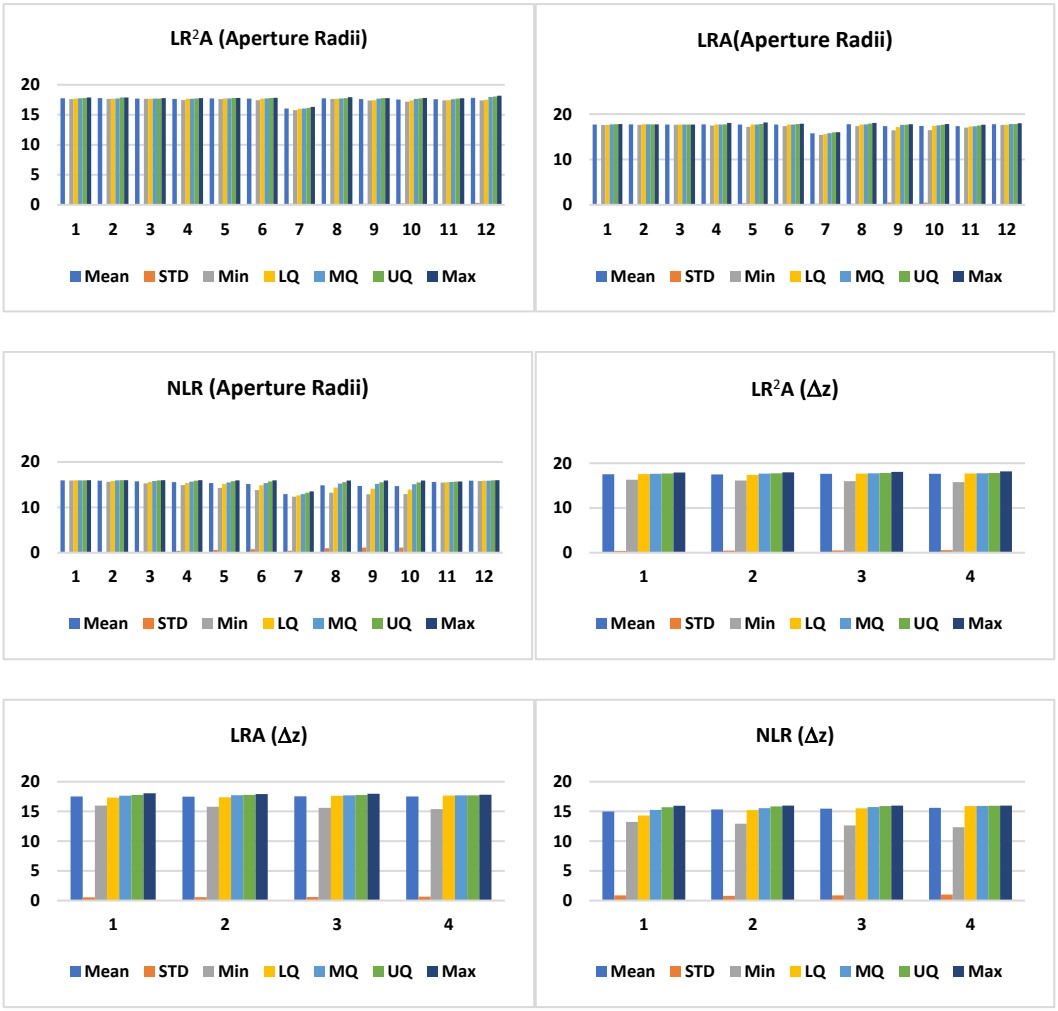

Figure S8: Graphical Plot Analysis of Peak signal-to-noise ratio (PSNR) with respect to deblurring

The Statistical Analysis of Table S7. represents the PSNR value with respect to deblurring and Graphical Plot Analysis of Fig S8 represents the Deblurring with respect to PSNR.

Table S8: Statistical Analysis of similarity index measure (SSIM) with respect to deblurring

SSIM	Range/Values	Mean	STD	Min	LQ	MQ	UQ	Max
LR²A	P100	0.60332	0.003091	0.5981	0.6021	0.6046	0.6047	0.6071
	P125	0.60856	0.000515	0.6079	0.6082	0.6086	0.6087	0.6094
	P150	0.60652	0.003134	0.6004	0.6075	0.6076	0.6084	0.6087
	P175	0.60418	0.004624	0.5982	0.599	0.6077	0.6078	0.6082
	P200	0.6033	0.004683	0.597	0.5986	0.6052	0.6076	0.6081
	P225	0.59984	0.007867	0.5888	0.5931	0.6014	0.6075	0.6084
	P25	0.40426	0.007485	0.3948	0.3982	0.4034	0.41	0.4149
	P250	0.6009	0.00661	0.5898	0.5996	0.6001	0.6071	0.6079
	P275	0.59402	0.011908	0.5764	0.5883	0.5913	0.6063	0.6078
	P300	0.59624	0.009771	0.5848	0.5855	0.5978	0.6051	0.608
	P50	0.51144	0.010089	0.4982	0.5052	0.5124	0.5133	0.5281
	P75	0.58034	0.005762	0.5732	0.579	0.5794	0.5794	0.5907
LRA	P100	0.60148	0.003461	0.5962	0.599	0.6025	0.6043	0.6054
	P125	0.60738	0.000412	0.6066	0.6074	0.6075	0.6077	0.6077
	P150	0.5989	0.018079	0.5632	0.6076	0.6077	0.6077	0.6083
	P175	0.59292	0.018324	0.5683	0.5734	0.6074	0.6075	0.608
	P200	0.58582	0.018185	0.5654	0.5695	0.5802	0.6069	0.6071
	P225	0.57996	0.025098	0.5514	0.552	0.5823	0.6069	0.6072
	P25	0.39028	0.010316	0.3758	0.3829	0.3905	0.3979	0.4043
	P250	0.5829	0.022363	0.5486	0.5715	0.5811	0.6063	0.607
	P275	0.56338	0.037375	0.5035	0.5461	0.5649	0.5956	0.6068
	P300	0.5632	0.036502	0.5067	0.5449	0.5617	0.5961	0.6066
	P50	0.50888	0.010544	0.4958	0.4994	0.5083	0.5179	0.523
	P75	0.57944	0.006522	0.5697	0.576	0.5795	0.5833	0.5887
NLR	P100	0.45426	0.004626	0.4456	0.4539	0.4561	0.4577	0.458
	P125	0.45142	0.016476	0.4234	0.4436	0.4577	0.4656	0.4668
	P150	0.44248	0.027609	0.4004	0.4233	0.4488	0.4662	0.4737
	P175	0.43338	0.034172	0.3887	0.4039	0.4339	0.4626	0.4778
	P200	0.42544	0.038108	0.3793	0.394	0.4181	0.4556	0.4802
	P225	0.41814	0.040336	0.3723	0.3866	0.4054	0.4457	0.4807
	P25	0.34872	0.008164	0.3374	0.3429	0.3488	0.3543	0.3602
	P250	0.41144	0.042485	0.3634	0.38	0.3981	0.4353	0.4804
	P275	0.40738	0.04369	0.3575	0.3769	0.394	0.4286	0.4799
	P300	0.40576	0.043385	0.3576	0.3759	0.3918	0.424	0.4795
	P50	0.41594	0.005124	0.4087	0.4128	0.4157	0.4191	0.4234
	P75	0.44264	0.004031	0.4366	0.4401	0.4429	0.4459	0.4477
LR²A	D-25	0.575583	0.054563	0.4149	0.588325	0.5974	0.60085	0.6086
	D-50	0.5753	0.058043	0.4034	0.583975	0.60075	0.605775	0.6079

	D-75	0.578742	0.061697	0.3982	0.596325	0.6067	0.608125	0.6094
	D-100	0.577333	0.063269	0.3948	0.591875	0.60765	0.607925	0.6087
LRA	D-25	0.556008	0.054912	0.3979	0.5458	0.56845	0.58855	0.6083
	D-50	0.564508	0.059151	0.3905	0.5641	0.58065	0.60375	0.608
	D-75	0.57435	0.065071	0.3829	0.5907	0.60265	0.60725	0.6077
	D-100	0.57445	0.067816	0.3758	0.589575	0.6067	0.606925	0.6077
NLR	D-25	0.404783	0.030956	0.3543	0.379225	0.39895	0.428375	0.4539
	D-50	0.417742	0.031233	0.3488	0.397075	0.4169	0.444375	0.4577
	D-75	0.43645	0.032931	0.3429	0.42745	0.4429	0.45915	0.4662
	D-100	0.454817	0.041531	0.3374	0.451225	0.47575	0.479975	0.4807

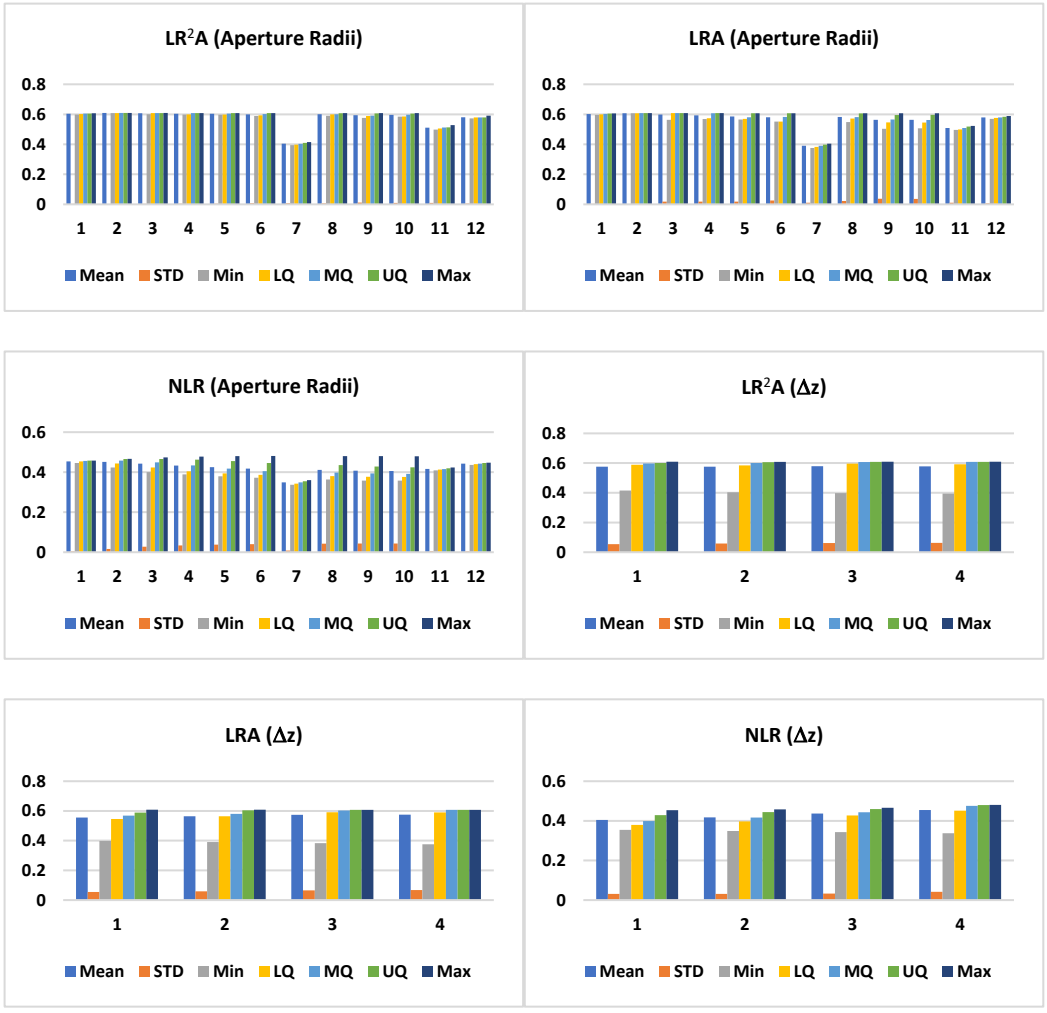

Figure S9: Graphical Plot Analysis of structural similarity index measure (SSIM) with respect to deblurring

The Statistical Analysis of Table S8. represents the SSIM value with respect to deblurring and Graphical Plot Analysis of Fig. S9 represents the Deblurring with respect to SSIM.

Table S9: Statistical Analysis of Visual information fidelity (VIF) with respect to deblurring

VIF	Range	Mean	STD	Min	LQ	MQ	UQ	Max
LR²A	P100	0.2522	0.006342	0.242	0.2489	0.2542	0.2556	0.2603
	P125	0.26268	0.000796	0.2614	0.2624	0.2626	0.2634	0.2636
	P150	0.26064	0.004848	0.2511	0.2627	0.2628	0.2628	0.2638
	P175	0.25844	0.006375	0.2478	0.2546	0.2629	0.2633	0.2636
	P200	0.25478	0.007528	0.2459	0.2482	0.2529	0.2631	0.2638
	P225	0.25274	0.010039	0.2397	0.2437	0.253	0.2628	0.2645
	P25	0.13286	0.003391	0.1278	0.1308	0.1332	0.135	0.1375
	P250	0.25474	0.007649	0.2443	0.2493	0.2537	0.2621	0.2643
	P275	0.24588	0.014492	0.2251	0.2354	0.2468	0.2578	0.2643
	P300	0.24744	0.011994	0.2335	0.2361	0.2463	0.2569	0.2644
	P50	0.16658	0.006476	0.1598	0.1624	0.1649	0.1675	0.1783
	P75	0.22092	0.006891	0.2123	0.2181	0.2187	0.2227	0.2328
LRA	P100	0.25436	0.004607	0.2475	0.2511	0.2552	0.258	0.26
	P125	0.2627	0.000725	0.2614	0.2626	0.2628	0.2633	0.2634
	P150	0.2535	0.020407	0.2132	0.2635	0.2635	0.2636	0.2637
	P175	0.24624	0.021484	0.2164	0.2245	0.2631	0.2634	0.2638
	P200	0.23794	0.021325	0.2148	0.2181	0.2311	0.2627	0.263
	P225	0.2334	0.026364	0.2031	0.2062	0.2321	0.2627	0.2629
	P25	0.1332	0.002596	0.1287	0.1322	0.1343	0.1348	0.136
	P250	0.23372	0.025131	0.1988	0.2179	0.2283	0.2606	0.263
	P275	0.21888	0.033196	0.1718	0.2001	0.2121	0.2475	0.2629
	P300	0.21776	0.032691	0.1751	0.1964	0.2083	0.246	0.263
	P50	0.17502	0.007111	0.1672	0.168	0.174	0.1808	0.1851
	P75	0.22946	0.006697	0.2202	0.2255	0.2288	0.2332	0.2396
NLR	P100	0.21652	0.004275	0.2088	0.2155	0.2181	0.2197	0.2205
	P125	0.2186	0.015689	0.192	0.2113	0.2239	0.2319	0.2339
	P150	0.21278	0.027463	0.1707	0.1936	0.22	0.2362	0.2434
	P175	0.20598	0.034667	0.1589	0.1773	0.2079	0.2362	0.2496
	P200	0.19928	0.039976	0.149	0.1671	0.1934	0.2314	0.2555
	P225	0.1938	0.042989	0.1451	0.157	0.1838	0.2239	0.2592
	P25	0.13402	0.003527	0.1286	0.1318	0.1348	0.1364	0.1385
	P250	0.18718	0.045171	0.1374	0.1496	0.1749	0.2153	0.2587
	P275	0.18358	0.046485	0.1324	0.147	0.1701	0.209	0.2594
	P300	0.18178	0.046345	0.1332	0.145	0.1669	0.2044	0.2594
	P50	0.17538	0.004944	0.1683	0.1721	0.1754	0.179	0.1821
	P75	0.20278	0.003022	0.1978	0.2013	0.2034	0.2055	0.2059
LR²A	D-25	0.232217	0.038176	0.1375	0.23845	0.24655	0.250875	0.2634
	D-50	0.23255	0.040299	0.1308	0.231225	0.25295	0.2563	0.2629
	D-75	0.238083	0.042846	0.1332	0.2412	0.25995	0.2636	0.2638

	D-100	0.2381	0.043641	0.135	0.234575	0.26295	0.2643	0.2645
LRA	D-25	0.215833	0.035962	0.1343	0.199175	0.21635	0.2394	0.2635
	D-50	0.224567	0.037413	0.1348	0.21115	0.22995	0.2571	0.2638
	D-75	0.237142	0.041237	0.1322	0.240875	0.25585	0.2627	0.2637
	D-100	0.2389	0.043354	0.1287	0.240675	0.2629	0.263	0.2636
NLR	D-25	0.173692	0.02666	0.1364	0.14895	0.1722	0.196575	0.2155
	D-50	0.189583	0.025866	0.1348	0.1737	0.1886	0.210925	0.2239
	D-75	0.209433	0.029425	0.1318	0.203625	0.2175	0.231525	0.2362
	D-100	0.227658	0.04087	0.1286	0.213025	0.2465	0.258825	0.2594

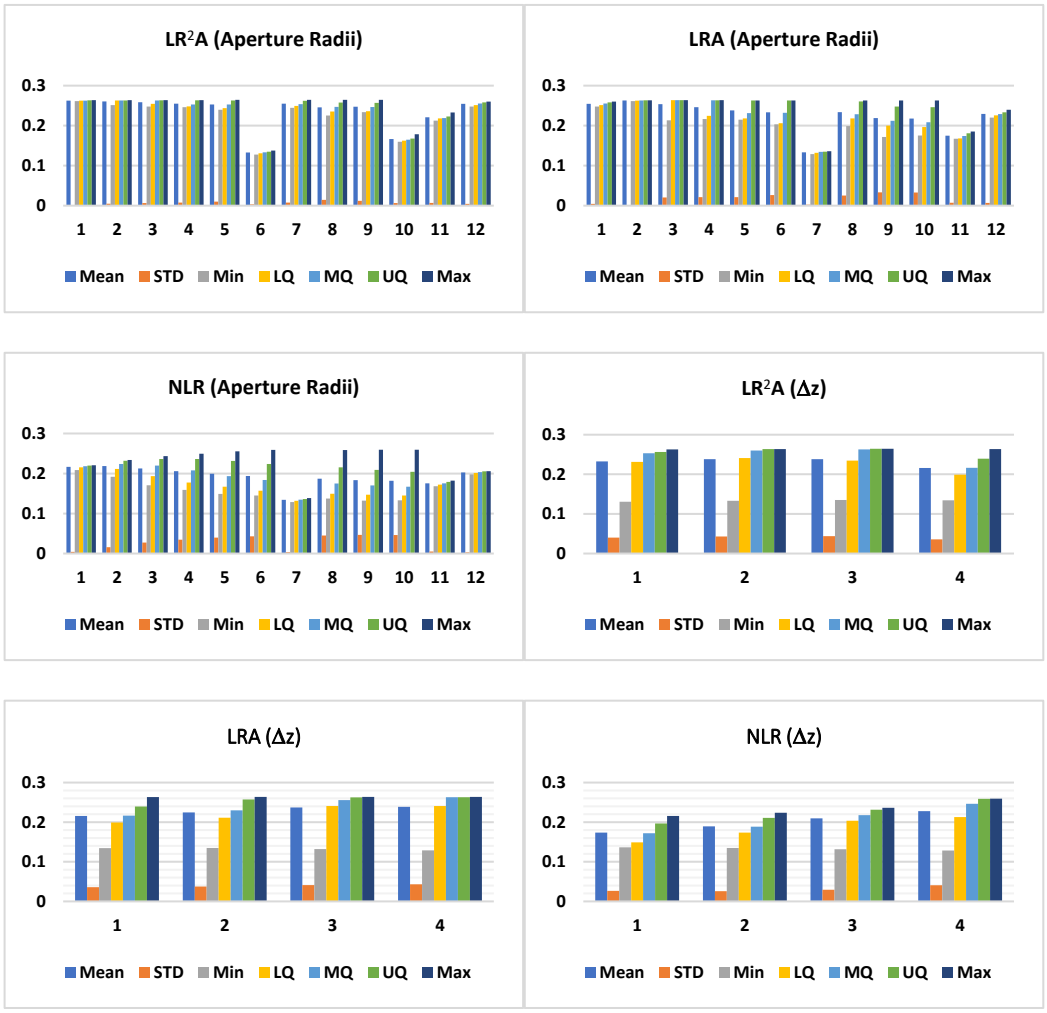

Figure S10: Graphical Plot Analysis of Visual information fidelity (VIF) with respect to deblurring

The Statistical Analysis of Table S9. represents the VIF value with respect to deblurring and Graphical Plot Analysis of Fig. S10 represents the Deblurring with respect to VIF.

Table S10: Statistical Analysis of Feature Similarity Index (FSIM) w.r.t deblurring

FSIM	Range	Mean	STD	Min	LQ	MQ	UQ	Max

LR²A	P100	0.7594	0.001252	0.7574	0.7587	0.7597	0.7603	0.7609
	P125	0.76058	0.000251	0.7603	0.7603	0.7606	0.7608	0.7609
	P150	0.76024	0.000304	0.7597	0.7602	0.7603	0.7604	0.7606
	P175	0.7601	0.000808	0.7586	0.7603	0.7603	0.7603	0.761
	P200	0.75914	0.000985	0.7579	0.7583	0.759	0.7602	0.7603
	P225	0.75852	0.002188	0.7544	0.7586	0.7591	0.7601	0.7604
	P25	0.62674	0.007535	0.6173	0.6201	0.6269	0.6318	0.6376
	P250	0.75916	0.001147	0.7572	0.7588	0.7593	0.7601	0.7604
	P275	0.75744	0.003309	0.7513	0.7574	0.7581	0.7601	0.7603
	P300	0.7584	0.001838	0.7551	0.7579	0.7592	0.7596	0.7602
	P50	0.70482	0.009208	0.6926	0.6989	0.7035	0.7102	0.7189
	P75	0.7466	0.005216	0.7395	0.7435	0.7461	0.7492	0.7547
LRA	P100	0.75822	0.001405	0.7558	0.7577	0.7587	0.7591	0.7598
	P125	0.76078	0.000402	0.7603	0.7606	0.7607	0.7608	0.7615
	P150	0.75768	0.006961	0.744	0.7605	0.7607	0.7608	0.7624
	P175	0.75486	0.006913	0.7464	0.7466	0.7604	0.7604	0.7605
	P200	0.7506	0.009326	0.7374	0.7429	0.7521	0.7603	0.7603
	P225	0.74886	0.011484	0.7349	0.7358	0.7531	0.7602	0.7603
	P25	0.61162	0.006536	0.6043	0.6051	0.6111	0.6167	0.6209
	P250	0.74978	0.010207	0.7352	0.7414	0.7517	0.7602	0.7604
	P275	0.74372	0.015915	0.7159	0.738	0.7499	0.7546	0.7602
	P300	0.74062	0.017155	0.7131	0.731	0.7446	0.7541	0.7603
	P50	0.69588	0.011129	0.681	0.6871	0.6962	0.7035	0.7116
	P75	0.74216	0.005209	0.7353	0.738	0.7422	0.7457	0.7496
NLR	P100	0.671	0.004685	0.6623	0.6703	0.6732	0.6744	0.6748
	P125	0.67068	0.015878	0.6439	0.6628	0.6766	0.6841	0.686
	P150	0.66484	0.025752	0.6263	0.646	0.6705	0.6873	0.6941
	P175	0.65852	0.031311	0.6181	0.6312	0.6583	0.6858	0.6992
	P200	0.65262	0.034976	0.6111	0.6231	0.6452	0.681	0.7027
	P225	0.64716	0.037424	0.6053	0.6172	0.6349	0.6735	0.7049
	P25	0.59012	0.005373	0.5828	0.5863	0.5899	0.5938	0.5978
	P250	0.64194	0.039245	0.5992	0.6121	0.6276	0.6653	0.7055
	P275	0.6397	0.039453	0.5985	0.6098	0.6248	0.6595	0.7059
	P300	0.63924	0.038637	0.6016	0.6089	0.624	0.6559	0.7058
	P50	0.63274	0.004286	0.6267	0.63	0.6326	0.6355	0.6389
	P75	0.6589	0.003158	0.654	0.6569	0.6595	0.6616	0.6625
LR²A	D-25	0.743525	0.036475	0.6318	0.7552	0.75825	0.759775	0.7609
	D-50	0.742567	0.03835	0.6269	0.75495	0.75905	0.75985	0.7606
	D-75	0.741842	0.040651	0.6201	0.7549	0.7601	0.7603	0.7604
	D-100	0.74075	0.041939	0.6173	0.752925	0.7602	0.7603	0.7604

LRA	D-25	0.732683	0.038419	0.6167	0.733925	0.74355	0.75385	0.7624
	D-50	0.736	0.041445	0.6111	0.742725	0.7508	0.759125	0.7607
	D-75	0.738275	0.045142	0.6051	0.750075	0.75895	0.760425	0.7607
	D-100	0.738267	0.046289	0.6043	0.750675	0.76025	0.7603	0.7608
NLR	D-25	0.631025	0.023698	0.5938	0.611525	0.62715	0.6499	0.6703
	D-50	0.643192	0.024802	0.5899	0.6269	0.64005	0.66225	0.6766
	D-75	0.6617	0.027813	0.5863	0.65665	0.6694	0.681775	0.6873
	D-100	0.6784	0.037507	0.5828	0.6684	0.69665	0.70505	0.7059

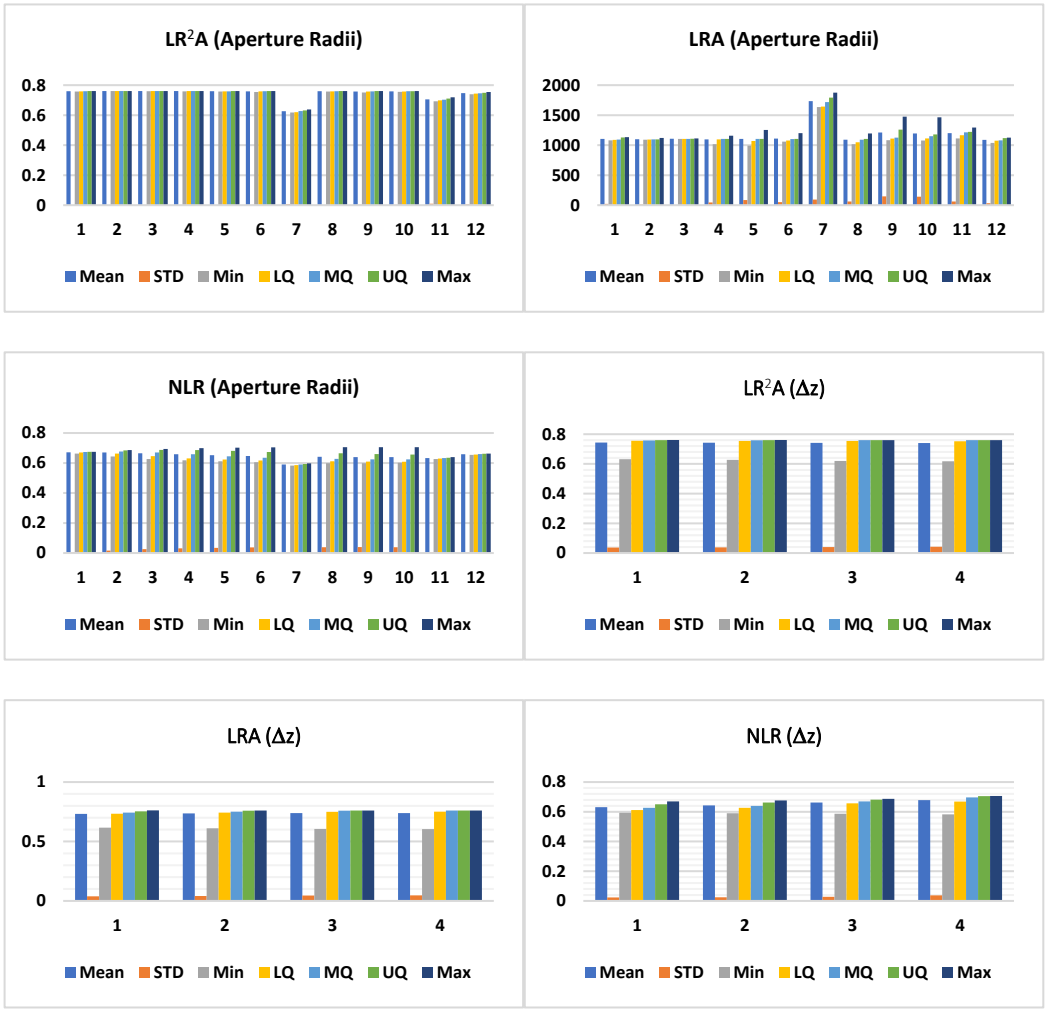

Figure S11: Graphical Plot Analysis of Feature Similarity Index (FSIM) with respect to deblurring

The Statistical Analysis of Table S10. represents the FSIM value with respect to deblurring and Graphical Plot Analysis of Fig. S11 represents the Deblurring with respect to FSIM.

Table S11. Statistical Analysis of Root-mean-square deviation (RMSE) with respect to deblurring .

RMSE	Range	Mean	STD	Min	LQ	MQ	UQ	Max
LR²A	P100	33.04746	0.347161	32.51899	32.84895	33.08194	33.27565	33.51178
	P125	32.98002	0.384956	32.49903	32.55729	33.12446	33.31909	33.4002
	P150	33.21981	0.152472	32.92955	33.22535	33.28688	33.30782	33.34944
	P175	33.39807	0.417275	32.97085	33.17554	33.33047	33.33547	34.17801
	P200	33.1171	0.274948	32.84879	32.8546	33.11796	33.17327	33.5909
	P225	33.2531	0.548755	32.76368	32.8129	33.17675	33.24475	34.2674
	P25	40.18287	0.81485	39.03224	39.73211	40.23921	40.44894	41.46185
	P250	33.0116	0.397458	32.3114	32.90651	33.09583	33.34257	33.40167
	P275	33.56892	0.663576	32.92199	32.95231	33.26612	34.23064	34.47354
	P300	33.83423	0.909058	32.81223	33.14183	33.47941	34.52388	35.21381
	P50	33.6998	0.542343	33.01172	33.23693	33.64268	34.22245	34.3852
	P75	32.77956	1.186274	31.4306	31.90631	32.22425	33.93121	34.40541
LRA	P100	33.23817	0.336072	32.86478	32.97789	33.07973	33.58624	33.68223
	P125	33.15789	0.152375	33.04137	33.06529	33.10225	33.12764	33.45289
	P150	33.25712	0.047808	33.22213	33.22811	33.23461	33.25123	33.3495
	P175	33.09806	0.704927	31.87117	33.12706	33.21222	33.24236	34.0375
	P200	33.20933	1.27301	31.5063	32.71115	33.21746	33.22263	35.38911
	P225	33.28368	0.73557	32.53658	32.81613	33.19817	33.22369	34.64383
	P25	41.6152	1.106208	40.43414	40.54809	41.43982	42.34514	43.30882
	P250	33.01937	0.915092	31.8907	32.39353	33.0379	33.21298	34.56173
	P275	34.72877	2.06585	32.9097	33.32303	33.53278	35.4698	38.40852
	P300	34.52895	1.961429	32.80536	33.34303	33.89986	34.33341	38.26311
	P50	34.64501	0.883453	33.36198	34.12075	34.82185	34.94863	35.97182
	P75	32.96727	0.49062	32.20195	32.78708	32.87544	33.41962	33.55227
NLR	P100	40.67752	0.127426	40.53525	40.58696	40.62976	40.75046	40.88516
	P125	41.0714	0.637157	40.56734	40.57186	40.73417	41.26073	42.22288
	P150	41.75549	1.261242	40.5212	40.71761	41.28716	42.35777	43.89373
	P175	42.61037	1.955456	40.53992	41.02354	42.07477	43.53222	45.8814
	P200	43.73187	3.072617	40.59619	41.43298	42.9135	44.54663	49.17005
	P225	44.88947	4.078091	40.672	41.92225	43.63763	46.16415	52.05131
	P25	57.64173	2.737291	53.91432	55.66685	57.55745	59.53896	61.53107
	P250	46.35129	5.435827	40.76934	42.44404	44.09886	48.78583	55.6584
	P275	47.22958	6.253811	40.78336	42.75346	44.47625	50.32715	57.80771
	P300	47.52235	6.280227	40.78851	42.94944	44.76199	51.43675	57.67508
	P50	42.35776	0.44173	41.77186	42.04189	42.32543	42.63654	43.01306
	P75	40.92044	0.254232	40.57264	40.72688	40.9222	41.11576	41.26469
LR²A	D-25	33.87549	1.653615	32.3114	33.13749	33.42113	33.79886	39.03224
	D-50	34.0075	1.906938	32.22425	33.09389	33.33083	34.40729	39.73211
	D-75	33.5631	2.131769	31.90631	32.7707	33.10389	33.30001	40.44894

	D-100	33.56448	2.441261	31.4306	32.8001	32.98202	33.20167	41.46185
LRA	D-25	34.06132	2.226	31.87117	32.89847	33.38456	34.68833	40.54809
	D-50	34.11606	2.402366	32.39353	32.86062	33.09617	34.48722	41.43982
	D-75	33.97098	2.577608	32.20195	33.0405	33.21743	33.57014	42.34514
	D-100	34.07759	2.803616	32.78708	33.21634	33.23303	33.34776	43.30882
NLR	D-25	45.61948	4.719348	40.58696	41.8466	44.03942	49.17116	55.66685
	D-50	43.77705	4.413854	40.53525	41.19592	42.61947	44.1932	57.55745
	D-75	43.14431	5.039722	40.56734	40.94706	41.67762	42.66577	59.53896
	D-100	42.65014	5.760656	40.5212	40.59011	40.7599	40.90756	61.53107

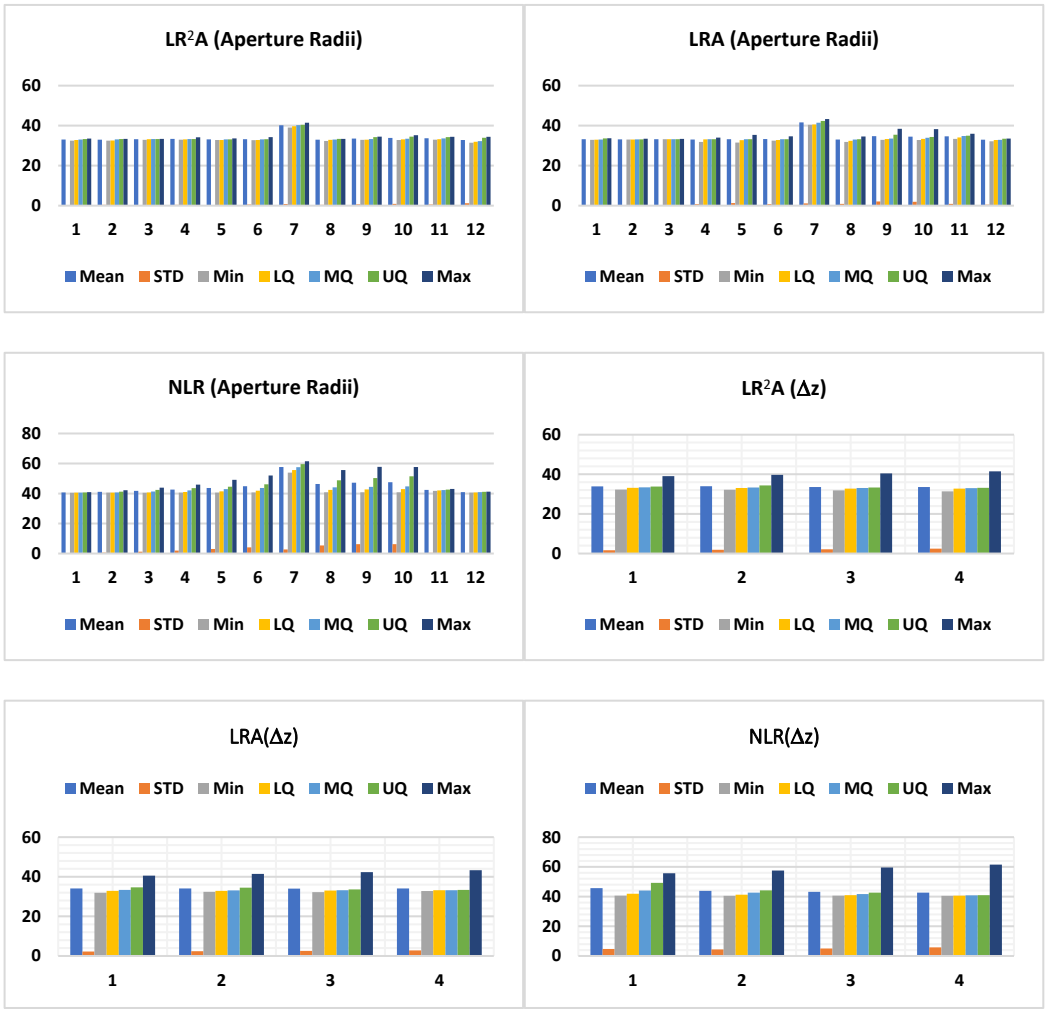

Figure S12: Graphical Plot Analysis of Root-mean-square deviation (RMSE) with respect to deblurring.

The performance measures based on aperture radii and axial aberrations were evaluated on different pre-trained deep learning networks and compared. To determine the best-performing models with descriptive statistics, image quality metrics such as PSNR, SSIM, FSI, and VIF were also used to evaluate the similarity between the ground truth and the reconstructed images. PSNR and SSIM measure pixel-level differences between the original and processed images, while FSI and VIF focus on the visual quality of the image.

Table S12: Overall Performance comparison w.r.t Image Similarity Metrics

Method	Range/Values	PSNR Mean	SSIM Mean	VIF Mean	FSIM Mean	RMSE Mean
	P100	17.74854	0.60332	0.2522	0.7594	33.04746
	P125	17.76634	0.60856	0.26268	0.76058	32.98002
	P150	17.70294	0.60652	0.26064	0.76024	33.21981
	P175	17.65704	0.60418	0.25844	0.7601	33.39807
	P200	17.73004	0.6033	0.25478	0.75914	33.1171
	P225	17.69528	0.59984	0.25274	0.75852	33.2531
LR²A	P25	16.05172	0.40426	0.13286	0.62674	40.18287
	P250	17.75808	0.6009	0.25474	0.75916	33.0116
	P275	17.61372	0.59402	0.24588	0.75744	33.56892
	P300	17.5467	0.59624	0.24744	0.7584	33.83423
	P50	17.57936	0.51144	0.16658	0.70482	33.6998
	P75	17.82424	0.58034	0.22092	0.7466	32.77956
	AVG	**17.5561667**	**0.5760767**	**0.2341583**	**0.742595**	**33.841045**
	P100	17.6985	0.60148	0.25436	0.75822	33.23817
	P125	17.71916	0.60738	0.2627	0.76078	33.15789
	P150	17.69312	0.5989	0.2535	0.75768	33.25712
	P175	17.73666	0.59292	0.24624	0.75486	33.09806
	P200	17.71176	0.58582	0.23794	0.7506	33.20933
	P225	17.68822	0.57996	0.2334	0.74886	33.28368
LRA	P25	15.74872	0.39028	0.1332	0.61162	41.6152
	P250	17.75864	0.5829	0.23372	0.74978	33.01937
	P275	17.33148	0.56338	0.21888	0.74372	34.72877
	P300	17.38022	0.5632	0.21776	0.74062	34.52895
	P50	17.34076	0.50888	0.17502	0.69588	34.64501
	P75	17.7701	0.57944	0.22946	0.74216	32.96727
	AVG	**17.4647783**	**0.5628783**	**0.2246817**	**0.734565**	**34.229068**
	P100	15.94376	0.45426	0.21652	0.671	40.67752
	P125	15.86102	0.45142	0.2186	0.67068	41.0714
	P150	15.72036	0.44248	0.21278	0.66484	41.75549
	P175	15.54926	0.43338	0.20598	0.65852	42.61037
	P200	15.33504	0.42544	0.19928	0.65262	43.73187
NLR	P225	15.12146	0.41814	0.1938	0.64716	44.88947
	P25	12.92562	0.34872	0.13402	0.59012	57.64173
	P250	14.8652	0.41144	0.18718	0.64194	46.35129
	P275	14.71732	0.40738	0.18358	0.6397	47.22958
	P300	14.66412	0.40576	0.18178	0.63924	47.52235
	P50	15.59262	0.41594	0.17538	0.63274	42.35776

	P75	15.89214	0.44264	0.20278	0.6589	40.92044
	AVG	**15.1823267**	**0.4214167**	**0.19264**	**0.6472883**	**44.729939**
LR²A	D-25	17.54262	0.575583	0.232217	0.743525	33.87549
	D-50	17.51184	0.5753	0.23255	0.742567	34.0075
	D-75	17.62915	0.578742	0.238083	0.741842	33.5631
	D-100	17.63333	0.577333	0.2381	0.74075	33.56448
	AVG	17.579235	0.5767395	0.2352375	0.742171	33.752643
LRA	D-25	17.50261	0.556008	0.215833	0.732683	34.06132
	D-50	17.49096	0.564508	0.224567	0.736	34.11606
	D-75	17.53038	0.57435	0.237142	0.738275	33.97098
	D-100	17.50658	0.57445	0.2389	0.738267	34.07759
	AVG	17.5076325	0.567329	0.2291105	0.7363063	34.056488
NLR	D-25	14.99195	0.404783	0.173692	0.631025	45.61948
	D-50	15.34378	0.417742	0.189583	0.643192	43.77705
	D-75	15.48088	0.43645	0.209433	0.6617	43.14431
	D-100	15.59524	0.454817	0.227658	0.6784	42.65014
	AVG	15.3529625	0.428448	0.2000915	0.6535793	43.797745

The Statistical Analysis of Table S11. represents the RMSE value with respect to deblurring and Graphical Plot Analysis of Fig. S12 represents the Deblurring with respect to RMSE.

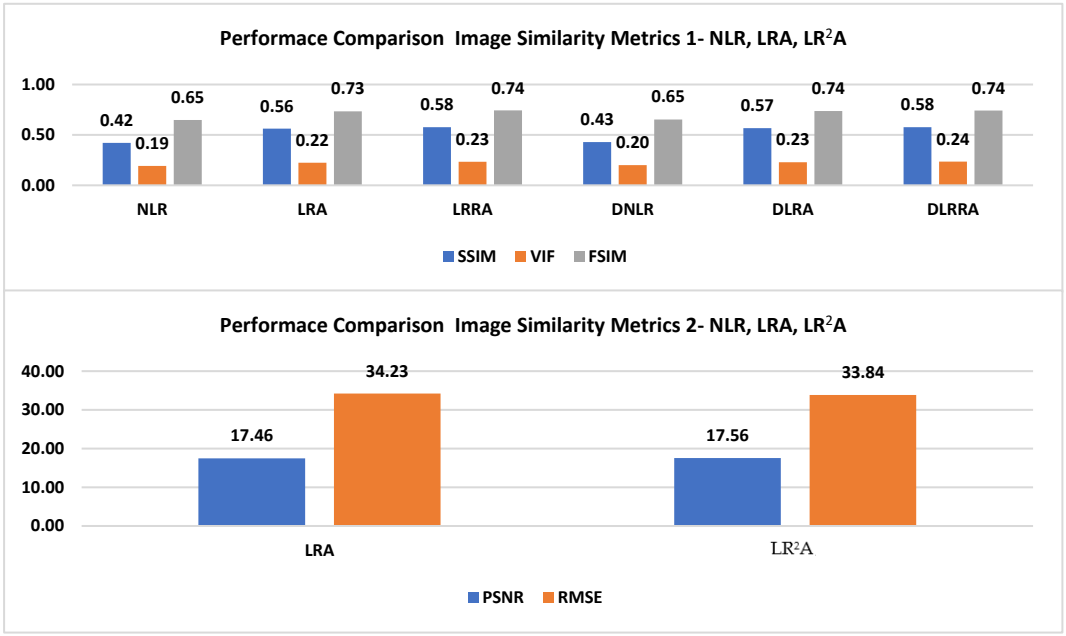

Figure S13: Graphical Plot Analysis of Performance Comparison - NLR, LRA, LR²A

Table S13: Performance comparison of Pre-trained Deep Learning models for NLR

Pre-trained_Models	Hits	Mean	STD	Min	LQ	MQ	UQ	Max
EFNETB0	64	9.1	0.9	7.3	8.6	9.5	9.9	10
IRV2	24	8.7	0.7	7.8	7.8	9	9.4	9.4
NNL	168	39.3	25	4.8	12.5	48.9	59.5	73
RS101	264	19.6	10	6.8	11.1	19.9	24.9	47.8
RN50	88	11.5	3	7.6	9.2	10.1	14.5	17

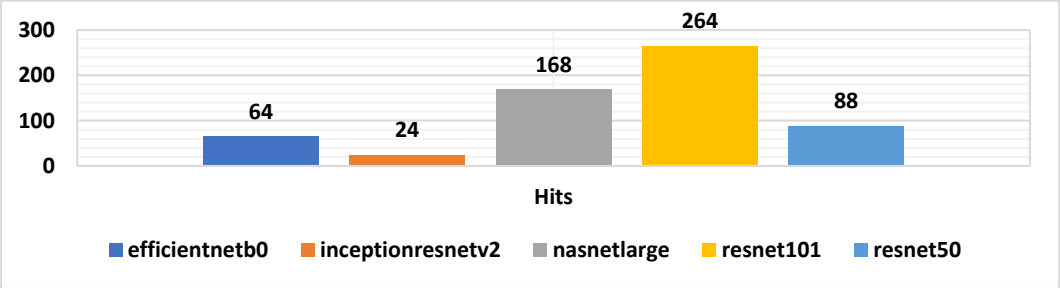

Figure S14: Graphical Plot Hit Analysis of Pre-trained Models Performance Comparison for NLR

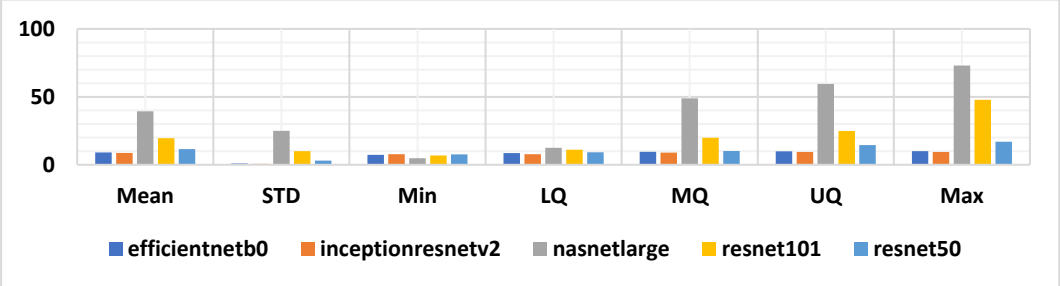

Figure S15: Descriptive Statistical Analysis of Pre-trained Models Performance Comparison for NLR

Table S14: Performance comparison of Pre-trained Deep Learning models for LRA

Pre-trained_Models	Hits	Mean	STD	Min	LQ	MQ	UQ	Max
DN53	40	24.2	8.7	11.2	18.2	25.9	30.3	35.4
EFNETB0	304	15.6	2.5	7.4	14.3	15.3	17.1	21.8
IRV2	296	38.8	7.8	20.8	35.8	38.3	40.5	65.5
NNMB	336	72.2	18.4	18.1	77.5	79.2	80.7	83.7
RS101	80	15.9	4.7	12.6	13.3	13.9	15.8	28
RN50	8	15.1	0	15.1	15.1	15.1	15.1	15.1

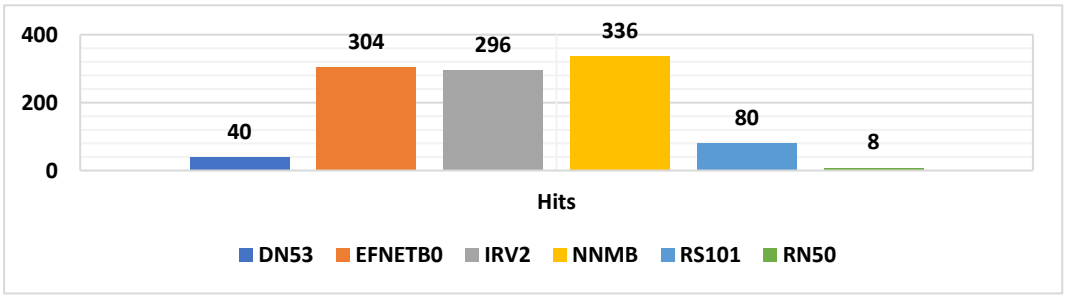

Figure S16: Graphical Plot Hit Analysis of Pre-trained Models Performance Comparison for LRA

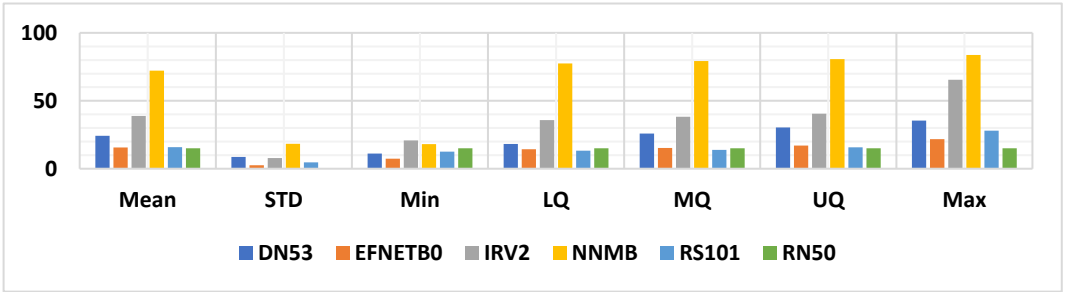

Figure S17: Descriptive Statistical Analysis of Pre-trained Models Performance Comparison for LRA

Table S15: Performance comparison of Pre-trained Deep Learning models for LR^{2}A

Pre-trained_Models	Hits	Mean	STD	Min	LQ	MQ	UQ	Max
DN53	64	19.3	6.1	7.9	15.7	19.2	23.8	27.8
EFNETB0	368	15	5.6	8.3	11.8	13.2	16.2	34.5
IRV2	352	37.1	12.9	12.8	31.7	35.2	38.1	75.5
NNL	368	73.5	10.5	39.7	73.2	77.5	80.6	86.7
NNMB	8	10	10	10	10	10	10	10
RS101	32	16.5	3	12.7	15	16.1	17.6	21
RN50	32	12.9	0.7	12.3	12.5	12.7	13.2	14

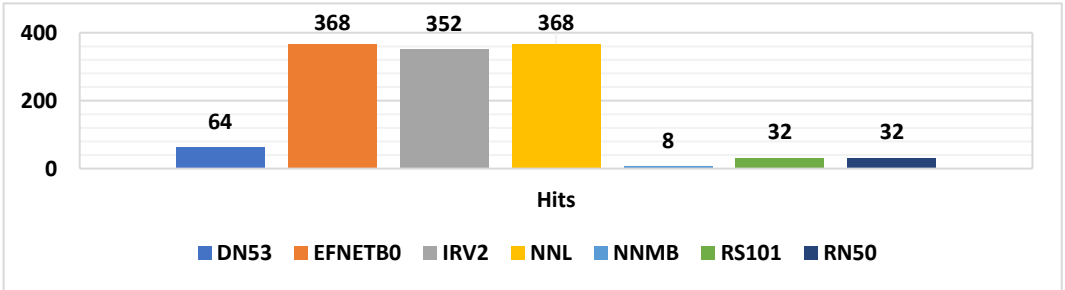

Figure S18: Graphical Plot Hit Analysis of Pre-trained Models Performance Comparison for LR^{2}A

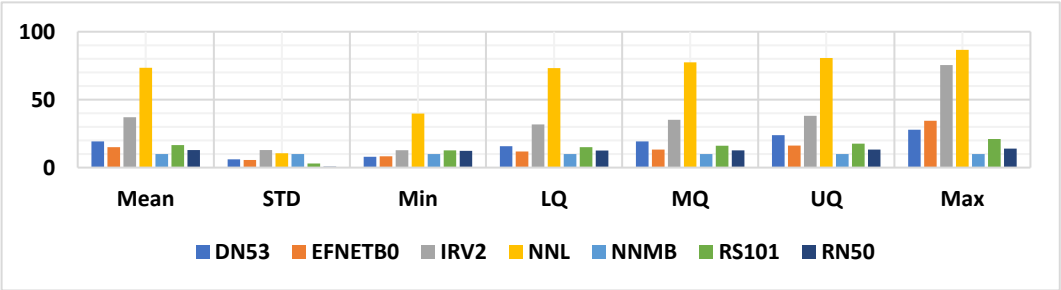

Figure S19: Descriptive Statistical Analysis of Pre-trained Models Performance Comparison for LR^{2}A

The NNL pre-trained model performed well with NLR method (mean=39.315) (Table S13), However, in the case of the LRA method, the NNMB model performed well with (mean=72.180) (Table S14), and the NNL model performed the best on average in the LR^{2}A method (mean=73.550) (Table S15).

DN53 was the only model that appeared in all three methods. NLR had the lowest mean values across all models (mean=88.258), and NNMB had the highest mean value in LRA (mean=72.180) but the lowest in LR^{2}A (mean=10.008). IRV2 had a relatively high mean value in both NLR (mean=8.747) and LRA (mean=38.763), while RS101 and RN50 had relatively consistent mean values across all methods.

The LR^{2}A method (figure. s18, s19) outperformed the LRA and NLR methods in total hits, with 1160, 1056, and 608 hits, respectively. However, the LR^{2}A method had the lowest mean value (154.91) and the highest standard deviation (45.17), indicating more variability in performance. The NLR method had the lowest standard deviation (39.56)(fig. s15) . The LR^{2}A method also had the highest minimum value (78.73) and maximum value (234.48). The median values were relatively close for all three methods, with LRA having the highest median value (172.56) (figure. s17), followed by LR^{2}A (155.01) and NLR (97.38).